



HAL
open science

Isotopes in groundwater as indicators of climate change

Philippe Négrel, Emmanuelle Petelet-Giraud

► **To cite this version:**

Philippe Négrel, Emmanuelle Petelet-Giraud. Isotopes in groundwater as indicators of climate change. Trends in Analytical Chemistry, 2011, 30 (8), pp.1279-1290. 10.1016/j.trac.2011.06.001 . hal-00677286

HAL Id: hal-00677286

<https://brgm.hal.science/hal-00677286>

Submitted on 7 Mar 2012

HAL is a multi-disciplinary open access archive for the deposit and dissemination of scientific research documents, whether they are published or not. The documents may come from teaching and research institutions in France or abroad, or from public or private research centers.

L'archive ouverte pluridisciplinaire **HAL**, est destinée au dépôt et à la diffusion de documents scientifiques de niveau recherche, publiés ou non, émanant des établissements d'enseignement et de recherche français ou étrangers, des laboratoires publics ou privés.

1
2 **ISOTOPES IN GROUNDWATER: INDICATORS OF CLIMATE**
3 **CHANGES**

4
5 **Philippe Négrel and Emmanuelle Petelet-Giraud**

6
7 BRGM, Metrology Monitoring Analysis Division
8 Avenue C. Guillemin, BP 36009, 45060 Orléans Cedex 02, FRANCE.

9 p.negrel@brgm.fr, e.petelet@brgm.fr,

10
11
12
13 Abstract: Isotopes of the water molecule ($\delta^{18}\text{O}$ and $\delta^2\text{H}$) are a well-used tool for investigating
14 groundwater origin and history, i.e. tracing the recharge conditions over time, processes
15 occurring during infiltration of the rain water towards aquifers and those issued from the
16 water-rock interaction and mixing of different waters. This paper proposes a review of several
17 large European aquifers (Portugal, France, UK, Switzerland, Germany, Hungary, Poland)
18 investigated in terms of the recharge conditions and the story of the groundwater at large
19 scale, involving recent, Holocene and Pleistocene components and eventually mixing between
20 them.

21
22
23
24
25 Keywords : hydrogeology, stable isotopes, Groundwater, Recharge, Climate change
26

27 **1 – Introduction**

28 Since several decades the use of isotopic methods in groundwater investigations is of great
29 acceptance among hydrogeologist and scientists scrutinizing groundwater resources and their
30 evolution in aquifer systems [1, 2]. Well-established techniques mainly applying stable
31 isotopes of the water molecule (hydrogen and oxygen) as tracers of water source have been
32 applied in water resource investigations and thus isotope hydrology and isotope hydrogeology
33 are great challenges since that time [3-6].

34 It is also clear and of great evidence either for scientists than end-users that groundwater is
35 one of the endangered resources of Europe. Groundwater, the main source of fresh water in
36 the majority of EU states, is under increasing threat from anthropogenic activities (industry,
37 intensive agricultural practices, mass tourism etc.). Because of over-exploitation, present
38 recharge cannot fully compensate for the increasing pumping, and groundwater resources are
39 declining in many of the important aquifers of Europe. Climate projections for Europe show
40 changes in precipitation and temperature patterns that are one of the key variables controlling
41 formation of groundwater resources [6]. Substantial decreases of precipitation have been
42 predicted for some parts of Europe while more rainfall is expected in the northern Europe.
43 The climate of Europe is diverse and characterized by large variations from north south and
44 east-west. In Southern Europe, global warming, will lead to a large reduction in recharge due
45 to the decrease in precipitation. This may lead to impacts on the water quality. In Central
46 Europe, continued depression of groundwater levels correlates with excessive use of water
47 resources. In the Atlantic regions and in Northern Europe increase in precipitation and
48 recharge and reducing of the unsaturated zone are expected as direct consequence of the
49 climate change. Thus, because aquifers may be subject of the climate change effect, which is
50 expected to decrease precipitation and recharge rates in large parts of Europe, there is no
51 general agreement on how to maintain a sustainable development of European aquifers in the
52 future [7]. The objective of this paper is to illustrate the past climates variations as well as
53 recharge over time and water origins using isotopic methods in groundwater investigations,
54 especially with stable isotopes of the water molecule ($\delta^{18}\text{O}$ and $\delta^2\text{H}$). Major continental
55 aquifer systems over Europe are used to illustrate complex stories of groundwaters from
56 infiltration to the aquifer through the processes that can affect their original signal.

57 **2- What is climate and climate changes?**

58 We are all living in areas of regional climate corresponding to the average weather in a place
59 over more than thirty years. The regional climate can be described by the temperatures over
60 the seasons, how windy it is, and how much rain or snow falls. The climate of a region
61 depends on many factors including sunlight amount, height above sea level, shape of the land,
62 and distance to the oceans. On the other hand, considering the entire earth, global climate is a
63 description of the climate as a whole including all the regional differences as average.

64 Climate variations and change, caused by external forcings, may be partly predictable,
65 particularly on the larger, continental and global, spatial scales. Because human activities,
66 such as the emission of greenhouse gases or land-use change, do result in external forcing, it
67 is believed that the large-scale aspects of human-induced climate change are also partly
68 predictable.

69 The climate system, comprising the atmosphere, the hydrosphere, the cryosphere, the land
70 surface and the biosphere is an interactive system as defined in the IPCC Report [8, 9]. This
71 system is forced or influenced by various external forcing mechanisms, the most important of
72 which are the Sun and the direct effect of human activities. In the climate system, the
73 atmosphere is the most unstable and reactive part of the system and its composition has
74 changed with the evolution of the Earth. The most variable component of the atmosphere is
75 water and because the transition between the various phases (vapour, cloud droplets, and ice
76 crystals) absorb and release lot of energy, water vapour is central for climate variability and
77 change. The hydrosphere is the component comprising all liquid surface and subterranean
78 water, both fresh (rivers, lakes and aquifers) and saline water (oceans and seas). Fresh water
79 runoff from the land to the oceans influences the ocean's composition and circulation but due
80 to the large thermal inertia of the oceans, they act as a regulator of the Earth's climate as well

81 as a source of natural climate variability, in particular on the longer time-scales. The
82 cryosphere, including the ice sheets, continental glaciers and snow fields, sea ice and
83 permafrost, derives its importance to the climate system from its albedo, low thermal
84 conductivity, large thermal inertia and its critical role in driving deep ocean water circulation.
85 Because of the large water amount stored in ice sheets, their volume variations are a potential
86 source of those of the sea level. Vegetation and soils control the Sun-atmosphere exchange of
87 energy. Part of the exchange induces heating of the atmosphere as the land surface warms,
88 part serves to evaporation processes inducing water returning back to the atmosphere.
89 Because the evaporation of soil moisture requires energy, soil moisture has a strong influence
90 on the surface temperature.

91 Many physical, chemical and biological interaction processes occur among the various
92 components of the climate system on a wide range of space and time scales, making the
93 system extremely complex. As an example, the marine and terrestrial biospheres have a major
94 impact on the atmosphere's composition through the uptake and release of greenhouse gases
95 by the biota. Similarly, the atmosphere and the oceans are strongly coupled and exchange,
96 among others, water vapour and heat through evaporation. This is part of the hydrological
97 cycle and leads to condensation, cloud formation, precipitation and runoff, and supplies
98 energy to weather systems.

99 However, climate varies by region as a result of local differences in these interactions [10].
100 Thus, some of the factors that have an effect on climate are changes in the amount of solar
101 energy, greenhouse gases, albedo of snow and ice and volcanic eruptions [11]. While the
102 weather can change in just a few hours, climate changes over longer timeframes. Any change,
103 whether natural or anthropogenic, in the components of the climate system and their
104 interactions, or in the external forcing, may result in climate variations. Climate has changed

105 in the past, is changing nowadays and will change in the future. The time scale of climate
106 change may vary from decades up to hundreds of million years.

107 **3- Why stable isotopes can trace climate changes?**

108 ***3.1 Trace the groundwater recharge***

109 Recharge of aquifer is mainly done by direct infiltration of rainwater, surface water or by
110 subsurface inflow, and thus primary originates from precipitation. In that way, it is necessary
111 to first constrain the signature of the recharge, i.e. of the rainfall. For the hydrosphere,
112 increasing global surface temperatures lead to changes in precipitation and atmospheric
113 moisture [12] and impact the recharge of the aquifers. By the 1950's, it has been observed that
114 stable isotopes of the water molecule in rainwater ($\delta^{18}\text{O}$ and $\delta^2\text{H}$, reflecting the ratio of heavy
115 and light isotopes of ^{18}O and ^{16}O , and ^2H and ^1H respectively) depend on several climatic
116 factors, including air temperature, rain amount, altitude and latitude of precipitations (e.g.
117 [13]). Thus combining this relationship between isotope ratios and climate and the well
118 established thermodependance, the isotopic signatures of the water molecule appear to be an
119 appropriate tool to study the past climates in various continental and marines archives.

120 The spatial and temporal variability of $\delta^2\text{H}$ and $\delta^{18}\text{O}$ of meteoric water results from isotope
121 fractionation effect accompanying evaporation/condensation processes. The laltitude effect
122 reflects the rainout process based on the Rayleigh fractionation/condensation model that
123 include two processes. Firstly, the formation of atmospheric vapour by evaporation in regions
124 with the highest surface ocean temperature and secondly, the progressive condensation of
125 vapour during transport to higher latitude. For coastal and continental stations in Europe, this
126 latitude effect is about : $\Delta^{18}\text{O} \approx -0.6\text{‰}/\text{degree}$ of latitude (GNIP data network; [14]). The
127 temperature is a key parameter that controls the $\delta^{18}\text{O}$ signatures (and thus $\delta^2\text{H}$), Yurstsever
128 [15] established the folowing relation based on amount-weigthed means $\delta^{18}\text{O}$ for North
129 Atlantic and European stations : $\delta^{18}\text{O} = 0.52 t - 15\text{‰}$. The temperature effect thus mainly

130 controls the seasonal variations of the isotopic signal in rainwater. The continental effect,
131 resulting in a progressive ^{18}O (and ^2H) depletion in rainwater with increasing distance from
132 the ocean, also largely controls the isotopic signature of precipitations. Over Europe, from
133 Irish coast to Ural Mountains, an average depletion of 7‰ is observed for $\delta^{18}\text{O}$, however the
134 extent to which a continental effect occurs also depends on the prevailing direction of the
135 movement of air masses. Finally, there is an altitude effect that is temperature-related, as the
136 temperature drops when altitude increases. All these parameters controlling the isotopic
137 signature in rainwater lead to the general relation between $\delta^{18}\text{O}$ and $\delta^2\text{H}$, defined as the
138 GMWL (Global Meteoric Water Line, [13]) : $\delta^2\text{H} = 8 * \delta^{18}\text{O} + 10$. The isotopic signal of the
139 recharge of aquifer, i.e. rainwater, over Europe is summarized as a map (Fig 1, [16])
140 reflecting well the continental and latitudinal effects. More detailed maps exist for European
141 countries, reflecting especially the local altitudinal effects (e.g. France: [17]; UK : [18, 19];
142 Spain: [20]; Italy: [21,22]).

143 The stable isotopes of the water molecule ($\delta^2\text{H}$ and $\delta^{18}\text{O}$) are generally measured using a
144 IRMS mass spectrometer with a precision of 0.1‰ vs. SMOW for $\delta^{18}\text{O}$ and 0.8‰ for $\delta^2\text{H}$.
145 Isotopic compositions are reported in the usual δ -scale in ‰ with reference to V-SMOW
146 according to $\delta_{\text{sample}} (\text{‰}) = \{(R_{\text{sample}} / R_{\text{standard}}) - 1\} \times 1000$, where R is the $^2\text{H}/^1\text{H}$ and $^{18}\text{O}/^{16}\text{O}$
147 atomic ratios. During the past decade, the ongoing development and evolution of laser gas
148 analyzers and laser spectroscopy presents an alternative to conventional IRMS and CF-IRMS
149 analysis of water isotopes O and H. In particular, the laser-based method is conceptually
150 simple [23] and may display some major advantages over the IRMS method: smaller sample
151 sizes, direct measurement of isotope ratios in the water vapour, avoiding the time-consuming
152 and sample preparations. On the other hand, the main disadvantage of laser spectroscopy
153 compared to IRMS is the lowering analytical flexibility because of the single gas isotopic
154 species of interest (e.g., water vapour, CO_2 , or CH_4). However, presently, if some studies tend

155 to demonstrate that laser technology for the measurement of liquid water isotopes yields
156 comparable or better accuracy to conventional IRMS and CF-IRMS analysis [24], others
157 highlight divergences and concern that exist about the capability of laser spectroscopy for the
158 analysis of liquid samples other than pure water due to the presence of organic compounds
159 [25].

160

161 ***3.2 What changes in the water molecule can be traced by O-H isotopes in aquifers?***

162 The isotopic composition ($\delta^2\text{H}$ and $\delta^{18}\text{O}$) of the water molecule can change (isotopic
163 fractionation) during its travel from the atmosphere, as rainwater, to groundwater, and
164 sometimes within the aquifer. These potential changes are controlled by evaporation and
165 exchange processes.

166 If the isotopic signatures are not affected by any process from surface to groundwater, the
167 measured isotope ratio in the aquifer strictly reflects the origin of the water (location, period
168 and process of recharge), i.e. the conditions prevailing at the moment of the recharge. Thus, as
169 the isotopic signature are highly thermo-dependent, the climate prevailing at the moment of
170 the recharge is preserved in the groundwater system, as a typical isotopic signature (under a
171 colder climate, the $\delta^2\text{H}$ and $\delta^{18}\text{O}$ values are depleted in heavy isotopes and are thus more
172 negative). If the isotopic signatures change along the groundwater paths, this traces the history
173 of the water, particularly the mixing, salinization and discharge processes [14]. Even if the
174 isotopic composition of groundwater is mainly inherited from atmospheric signal, there is
175 some cases where reactions between groundwater and the rock matrix or gases or surface-
176 subsurface processes such as evaporation, can modify the original meteoric signatures [14, 4].

177

178 **4 - Recharge and residence time assessment of groundwater in the Adour Garonne**
179 **district (S.W. France) through stable isotopes of the water molecule**

180 The Adour-Garonne district covers 116 000 km² (1/5th of French territory). It is limited by the
181 Massif Central and Montagne Noire to the east, by the Armorican Massif to the north, by the
182 Pyrénées Mountains to the south and by the Atlantic Ocean to the west (Fig. 2). In this
183 district, the Eocene sands water body (a multi-layer system) constitutes a series of major
184 aquifers used for drinking water supply (6.7 million inhabitants), agriculture irrigation and
185 thermo-mineral water resource [26] and is composed by sandy Tertiary sediments alternating
186 with carbonate deposits. The Eocene aquifer system presents a high permeability and a
187 thickness of several tenths of meters to a hundred meters and is constituted by at least five
188 aquifers: Paleocene, Eocene infra-molassic sands (IMS), early Eocene, middle Eocene, late
189 Eocene. Groundwater recharge may occur to the east by the edge of the Massif Central, to the
190 south by the edge of the Pyrénées and by inflow from the Paleocene aquifer.

191 The $\delta^{18}\text{O}$ values of the ground waters fall in the range -5.6 to -10.6‰ vs. SMOW, with the
192 $\delta^2\text{H}$ values varying between -34.3 and -72.3‰ vs. SMOW [2]. There is no relationship
193 between $\delta^{18}\text{O}$ and $\delta^2\text{H}$ values and the salinity with a correlation coefficient R close to 0.30
194 and 0.45 between salinity and $\delta^{18}\text{O}$ - $\delta^2\text{H}$ values respectively. All the analysed waters (Fig. 3)
195 plot on or near the global meteoric water line GMWL [13].

196 The groundwater data present a wide range of stable isotopic composition ($\delta^2\text{H}$, $\delta^{18}\text{O}$) both
197 between the different aquifers and within a single aquifer (Fig. 3). Comparing independently
198 each aquifer level sampled in low and high flows of a same hydrological cycle, it appears:

199 *Palaeocene aquifer* collected NW-SE along the Pyrenees border presents a large variation in
200 the $\delta^{18}\text{O}$ and $\delta^2\text{H}$ signature, agreeing with that observed in the district. Such heterogeneity in
201 the $\delta^{18}\text{O}$ and $\delta^2\text{H}$ signatures for the Palaeocene aquifer reflects a variable recharge, either in
202 space and time. The most depleted value correspond to a water recharged with a colder

203 climate than the present one (> 10 000 y), the likeness in the $\delta^{18}\text{O}$ and $\delta^2\text{H}$ signatures along
204 the hydrological cycle confirms a homogeneous aquifer system without any water input with a
205 different signature between the two periods. This means that the aquifer is mostly confined
206 with no significant recharge.

207 *Lower Eocene aquifer* was essentially collected in the northern part of the district (Fig. 3).
208 The $\delta^{18}\text{O}$ and $\delta^2\text{H}$ signatures are less variable than those of the Paleocene aquifer and fall in
209 the middle range observed as a whole. The values are consistent along the hydrological cycle
210 and are more depleted compared to the present rainwater input in the Massif Central,
211 reflecting an older recharge which could have occurred under colder climate. This means that
212 the aquifer is probably semi-confined.

213 *Middle Eocene aquifer* has been largely sampled in the northern part of the district and
214 presents a large range of $\delta^{18}\text{O}$ and $\delta^2\text{H}$ signatures among which the most enriched values, very
215 close to that of the rain inputs observed in Dax, reflecting a modern recharge. Most of the
216 samples show depleted values that reflect a recharge under colder climate. In between these
217 two groups, a third group with intermediate values corresponds either to a mixture between
218 the two previous groups or to close pockets (e.g. small confined part of the aquifer). The large
219 variation of the point EM4 between the two surveys surely reflects hydrological conditions
220 that differ from one survey to the other.

221 *Upper Eocene aquifer* was sampled in 4 locations in the northern part of the district along a
222 NW-SE profile. Although having similar signature between the two surveys, they display
223 either enriched or depleted values. ES-3 is enriched while ES-4 is depleted (recharge under
224 colder climate) and ES-2 displays a signature close to present day rain water in the Massif
225 Central.

226 *Infra Molassic Sand aquifer* was largely collected in the southern part of the district along a
227 W-E profile and displays a large range of $\delta^{18}\text{O}$ and $\delta^2\text{H}$ signatures. SIM2 and SIM8 have a

228 signature close to those of rainwater in Dax and Massif Central. SIM2 is a shallow bore well
229 (58 m) and a modern recharge is compatible with the observed values. On the contrary, SIM8
230 is a 1400 m depth bore well screened between 1030 and 1040 m and the water is the most
231 saline of the district (TDS up to 2.5 g.L⁻¹). The $\delta^{18}\text{O}$ and $\delta^2\text{H}$ signature, suggesting a modern
232 recharge, may results in a rapid circulation of the groundwater in the system. As for the
233 remaining points, they are depleted in ¹⁸O and D compared to rainwater, reflecting a recharge
234 under colder climate and a semi confined status for the aquifer.

235 Taken as a whole, the enriched samples clearly correlate with the present day recharge as
236 measured in Dax and Massif Central. The most enriched waters (EM1, EM2, ES3) originate
237 from the north of the area, in the vicinity of the Gironde estuary and present signatures quite
238 similar to that of present day coastal precipitations (mean weighted rain in Dax). Samples
239 SIM2 and 8 also show an enriched signature that can be related to the modern recharge. At the
240 opposite, the most depleted sample (P3) originates from the Paleocene aquifer (860 m depth),
241 and may reflect an old recharge as its signature is clearly lower than that of present-day
242 precipitations from the Massif Central or Pyrenees. The groundwater presents a wide range of
243 variation along the global meteoric water line which excludes significant evaporation of
244 infiltrating waters and any continental effect on the stable isotope composition. These
245 variations cannot be easily correlated with the data spatial location, and are probably mostly
246 due to the period and location of the recharge of the aquifer. The most depleted sample of
247 IMS (SIM4) is located in the eastern border of the basin and originates from 177 m depth, it
248 may represent an old recharge (as the estimated age of some ground waters are close to 16–35
249 ka using ¹⁴C, [26]).

250 **5 – Stable isotope in some European large aquifers**

251 Variations of the $\delta^{18}\text{O}$ and $\delta^2\text{H}$ signature in the Eocene aquifer system from the Adour-
252 Garonne district in SW France can be related to changes in the recharge over various climatic

253 periods, from present day to old (e.g. up to 35 ka). Similar behavior can be revealed by several
254 studies of groundwaters in aquifers and such significant isotopic depletion of groundwaters
255 may be due to a lower recharge temperature at the time of infiltration [27]. We will consider
256 several cases of illustration in European aquifers as summarized in Figure 4 for which the
257 authors have investigated groundwater as archive of climatic changes or as being a reflection
258 of a more recent recharge period.

259

260 ***5.1. Aquitaine Basin***

261 The Aquitaine basin considered in the study by Le Gal La Salle et al. [28] and Jirakova et al.
262 [29]) occupies an area of 25,810 km² and extends essentially in the northern part of the
263 Adour-Garonne area (Poitou-Charentes district) and is limited to the west by the Atlantic
264 Ocean. Lower and Middle Jurassic carbonate formations make up the deepest aquifer of the
265 northern part of the Aquitaine Basin investigated in these studies. Reported in the $\delta^{18}\text{O}$ vs.
266 $\delta^2\text{H}$ graph (Fig.5), data plot in the upper range of values measured for the whole Aquitaine
267 Basin (see this work, §4 and André [26]).

268 Groundwaters with a wide range of $\delta^{18}\text{O}$ values (-4.9 to -7.4‰) and $\delta^2\text{H}$ (-35 to -48‰) plot
269 along the GMWL reflecting the meteoric origin (Fig.5, [28]). Some of the groundwaters are
270 significantly enriched or depleted in comparison with modern waters ($\delta^{18}\text{O}$ around - 5.7‰ and
271 $\delta^2\text{H}$ around -36‰). Considering the repartition of the values, Enriched stable isotopes in
272 groundwaters in the southwest part of the area were evidenced while groundwaters are either
273 depleted or similar to modern recharge northeastward [28]. The heterogeneity of the recharge
274 conditions in the area are attested by the observed variations and may be due to climate,
275 temperature or infiltration changes even if the authors do not preclude mixing with enriched
276 waters (e.g. seawater) in the deeper part of the basin. However, groundwaters having a
277 depleted value compared to the modern recharge plead in favor of a large palaeorecharge of

278 the aquifer that occurred during a colder period, possibly the last glaciation or deglaciation
279 periods.

280 Considering a larger area in the Poitou-Charentes district, Jirakova et al. [29] show an entire
281 range of stable isotope values from -7.7‰ to -4.9 ‰ for $\delta^{18}\text{O}$ and -52.3‰ to -29.6‰ for $\delta^2\text{H}$
282 that agree with the study of Le Gal La Salle [28] concerning the heterogeneity of the recharge
283 conditions as demonstrated in the $\delta^{18}\text{O}$ vs. $\delta^2\text{H}$ diagram (Fig.5). Enlarging the area confirms
284 the existence of depleted $\delta^{18}\text{O}$ and $\delta^2\text{H}$ values and suggests lower temperatures during the
285 recharge period. This type of waters represents the palaeorecharge under cold climatic
286 conditions during the late Pleistocene period and was clearly separated from those of the
287 Holocene. The modelling of the water residence time, using ^{14}C , showed Holocene waters
288 with enriched values (around -6‰ and -38.5‰ for $\delta^{18}\text{O}$ and $\delta^2\text{H}$, respectively) with
289 radiocarbon ages up to 10 ka B.P. On the other hand, the groundwaters having depleted values
290 (around -7.4‰ and -48‰ for $\delta^{18}\text{O}$ and $\delta^2\text{H}$, respectively) have radiocarbon ages between 20
291 and 15 ka B.P. that corresponds to the cold recharge.

292

293 **5.2 Paris Basin**

294 Moving north of the Aquitaine Basin, the Paris basin is the second major sedimentary basin in
295 France with an extend of around 600 km in diameter and more than 3000 m of sediment
296 deposits. The Dogger aquifer (200-300 m, predominantly limestone), confined between the
297 Liassic and Upper Callovian marls was studied by Matray et al. [30]. The Cretaceous Chalk
298 aquifer (700m of fine grained limestone) either confined or unconfined is extensively
299 exploited for drinking water and irrigation and was studied by Kloppmann et al.[31].

300 Groundwater samples from the recharge zone of the *Dogger aquifer* mimic the stable isotope
301 composition of the present day rain waters, indicating a recent meteoric origin (Fig.5). The
302 rest of the groundwater plot on the right the meteoric water line with low variations in the $\delta^2\text{H}$

303 and $\delta^{18}\text{O}$ (range -40 up to -30‰ for $\delta^2\text{H}$ and $\delta^{18}\text{O}$ in the range -6 up to -3‰). In this part of
304 the basin, the water temperature and salinity are high but seem to have no impact on the stable
305 isotope signatures. The authors discussed the possible isotope exchange with the carbonate
306 matrix for oxygen, and with H_2S for deuterium, but they argued that such processes cannot be
307 the major one controlling the groundwater isotope values. Important mixing processes are
308 responsible of both the stable isotope composition and salinity of the groundwater in the
309 Dogger aquifer and successive mixings between sedimentary brines with several meteoric
310 waters led to the observed isotope compositions of the groundwater. The authors argue for
311 percolation of meteoric water, dissolution of halite in the Triassic aquifer that generate a brine
312 that mixed with a residual primary brine, then migrated via vertical faults into the Dogger
313 aquifer.

314 Stable isotopes in the confined groundwaters of the Paris Basin *Chalk aquifer* plead in favour
315 of a recharge during Holocene time with a water component related to Pleistocene ages in the
316 deepest confined part of the aquifer. The observed depleted values in the confined part of the
317 aquifer can be related to a lower recharge temperature at the time of infiltration. On the other
318 hand, the influence of the continental effect affects the stable isotope composition of Chalk
319 groundwaters. The observed depletion of the stable isotopes in the unconfined groundwaters
320 from west to east mimics the one that could be observed in rainfall when air masses
321 penetrated a continental area. Long term changes in the input function related to climatic
322 evolution yield to the lowermost $\delta^2\text{H}$ - $\delta^{18}\text{O}$ values in the confined aquifer as well enriched
323 values in the unconfined aquifer originates from fractionation processes due to variation in the
324 recharge signal (e.g. the rain input).

325

326 ***5.3 London Basin***

327 In United Kingdom, the Chalk aquifers were studied by Hiscock et al. [32] in the Norfolk area
328 (eastern England), by Dennis et al. [33] in the London Basin (SE England) and by Elliot et al.
329 [34] in the London and the adjacent Berkshire Basin (east of the London Basin). The geology
330 consists of Cretaceous Chalk overlain by Tertiary clastic deposits with a thickness of more
331 than 400 m in the Norfolk area and up to 250 in the London Basin.

332 $\delta^{18}\text{O}$ - $\delta^2\text{H}$ values fall within the range of -8‰ to -6.6‰ and -55‰ to -43‰ respectively and
333 all data plot on, or close to the global meteoric water line as illustrated in Fig.5.

334 Both studies argue that the evolved Chalk waters typically show enriched isotopic signatures
335 that might be compared to the recharge temperatures determined through noble gas
336 investigations. This may reflect the mixing of relatively young groundwater in the fissures
337 with older groundwater in the matrix. The $\delta^{18}\text{O}$ - $\delta^2\text{H}$ variation along the meteoric water line
338 was related by all studies to the complexity of the recharge over time and mixing processes in
339 the aquifer. The conceptual model for the Chalk aquifer suggests that the water evolved from
340 connate Cretaceous marine water repeatedly mixed with fresh meteoric water since the Late
341 Tertiary. The present day conditions reflect such mixing with palaeowater recharged during a
342 cold period.

343

344 ***5.4 Lorraine Basin***

345 Moving eastward of the Paris Basin, the lower Triassic in eastern France is mainly
346 represented by sandstones and conglomerates and the extent of the Triassic aquifer reaches
347 3000 km² for the unconfined and 25,000 km² for the confined part. In the $\delta^2\text{H}$ vs. $\delta^{18}\text{O}$ graph
348 (Fig.5), data are scattered between two extreme values, the most enriched values correspond
349 to recent waters close to the recharge zone and reflect the values of modern rainfall [35]. On
350 the other hand the depleted values may correspond to a cooler recharge regime during the
351 Holocene.

352

353 ***5.5 Germany: Gorleben and Laegerdorf Basins***

354 Moving more eastward, the salt structure of Gorleben–Rambow in Germany, crossing the
355 Elbe river about 100 km upstream of Hamburg has been investigated in detail since past
356 decades with around 400 boreholes [36]. In this frame, all analysed fluids plot on the global
357 meteoric water line. The shallow groundwaters show $\delta^{18}\text{O}$ values of -8 to -8.5 ‰ and $\delta^2\text{H}$ of
358 -56 and -60 ‰ (Fig. 5), in the typical range of meteoric waters and have been identified as
359 modern on the base of their ^{14}C and ^3H contents. Most saline waters are depleted with respect
360 to shallow groundwater by up to 20 ‰ in ^2H and 2 ‰ in ^{18}O . The lowest observed values are
361 -72 ‰ ($\delta^2\text{H}$) and -10.3 ‰ ($\delta^{18}\text{O}$) for samples with salinities around 50 g/l. A group of highly
362 saline groundwaters show stable isotope contents in the range of shallow freshwaters. The
363 depletion of most of the deep saline groundwaters can be explained by a significant
364 contribution of Pleistocene recharge probably through meltwater infiltration during or shortly
365 after the last glaciation, this interpretation being in agreement with radiocarbon data.
366 Intermediate stable isotope contents are due to mixing between Holocene and Pleistocene
367 components leading to the large scatter of the reported values.

368 Also in Germany, Kloppmann et al.[31] presented isotope data in chalk groundwater (Fig. 5).
369 The Laegerdorf Chalk outcrop (Campanian- Maastrichtian) is exploited up to a 90 m depth.
370 The $\delta^2\text{H}$ and $\delta^{18}\text{O}$ values plot along the meteoric water line but with higher values than in
371 Gorleben. Kloppmann et al. [31] related the most depleted values in Laegerdorf to a
372 temperature effect.

373

374 ***5.6 Pannonian Basin***

375 Moving more eastward, the Pannonian Basin is a large area formed mainly during the late
376 Tertiary and Quaternary periods and covering 100,000 km² in southeast Hungary. The

377 hydrogeological system is a multilayer aquifer system with an intermediate flow regime in the
378 Pleistocene sediments that concerns local to regional scale and a deeper system, lower than
379 2500 m that concerns the regional scale.

380 Groundwaters plotted in a $\delta^2\text{H}$ and $\delta^{18}\text{O}$ graph define 2 groups (Fig.5, [37]). One group,
381 corresponding to the deeper part of the aquifer (500 – 2500 m, $T>40^\circ\text{C}$) shows a weak range
382 in $\delta^2\text{H}$ and $\delta^{18}\text{O}$ and plots close to the global meteoric water line. This suggests that
383 infiltration occurred during the same and probably the last cold period that occurred between
384 70,000 and 12,000 years BP. The other group of waters plots to the right of the global
385 meteoric water line and the shift of the $\delta^2\text{H}$ and $\delta^{18}\text{O}$ is not related to an evaporation process
386 but to mixing between old waters with water enriched in heavy isotopes [37]. The origin of
387 the enriched waters is suspected to be from oil field water, squeezed from the Pannonian
388 layers underlying the aquifer.

389

390 ***5.7 Poland Basin***

391 The Malm aquifer (limestones, sandstones and marls) in southern Poland around Cracow is
392 the most eastward of the investigated aquifers we illustrate in this study. This aquifer is
393 intensively exploited and this aquifer serves as a major strategic reserve of potable water for
394 the 1 million inhabitants of Cracow. The Malm aquifer is driven by numerous faults, graben
395 and horsts and as a consequence of this complex geology, flow pattern and ages of water are
396 poorly constrained. Based on several tools like nobles gases, tritium and carbon isotopes,
397 Zuber et al. [38] defined a range of water ages on the confined and unconfined part of the
398 aquifer from modern period to glacial waters, and glacial waters partly mixed with older water
399 (e.g. before 15ka BP).

400 In the $\delta^2\text{H}$ and $\delta^{18}\text{O}$ graph illustrated in Fig. 5 groundwaters plot along the GMWL. Modern
401 waters show enriched $\delta^2\text{H}$ - $\delta^{18}\text{O}$ values, in agreement with the mean annual precipitation.

402 They are either from present day (e.g. containing tritium) or from pre-bomb time (e.g. free of
403 tritium). More the waters are old, more they plot with depleted $\delta^2\text{H}-\delta^{18}\text{O}$ values and their
404 status (glacial-Holocene transition period waters and glacial waters) is constrained by the
405 $\delta^2\text{H}-\delta^{18}\text{O}$ values and noble gases temperatures. The older waters show the largest $\delta^2\text{H}-\delta^{18}\text{O}$
406 depleted values and are related to other recharge areas, or deeper origin than the glacial waters
407 [38].

408

409 ***5.8 Portugal***

410 Moving south-westward Europe, in the south Portugal, the Sado sedimentary basin is made of
411 Eocene (sandstone and carbonate), Miocene (conglomerates, limestones and sandstones) and
412 Pliocene (conglomerates and sands) sediments [39]. Within the Sado basin the Plio-Miocene
413 and the Eocene are the two identified aquifer systems. The two aquifers have similar $\delta^2\text{H}-$
414 $\delta^{18}\text{O}$ values with as example -5.0 to -4.0‰ in the Eocene aquifer and -5.0 to -4.6‰ in the
415 Plio-Miocene aquifer for the $\delta^{18}\text{O}$ (Fig. 5). Values are depleted along the flow path is
416 observed as shown by the Plio-Miocene, which is more depleted near the northern limit of the
417 basin when compared to the southern. According to the range in the ^{14}C ages for the
418 groundwater and the $\delta^2\text{H}-\delta^{18}\text{O}$ values in the Plio-Miocene and Eocene aquifers, Galego-
419 Fernandes and Carreira [39] argue for infiltration processes of the Eocene waters under
420 climatic conditions different from the modern ones.

421

422 ***5.9 A highly complex aquifers system: the Switzerland example***

423 In the middle of the Europe, the northern Switzerland is composed of three main sedimentary
424 stratigraphic groups from Tertiary to Permo-Carboniferous that include large aquifers,
425 potentially locally connected through tectonic accidents. These sediments contain several
426 aquifers, it is composed of sandstone (Tertiary-Malm group) and Malm limestones; the upper

427 Muschelkalk consist of limestones and dolomites; and the lower Triassic-Permian group
428 consists of clastic sediments. The two other aquifer systems are the Quaternary cover, largely
429 impacted by anthropogenic activities, and the crystalline basement where water circulations in
430 the crystalline basement are mainly controlled by tectonic fractures [40]. The synthesis
431 present waters sampled in the beginning of the 80's (Fig. 5). Waters from Quaternary,
432 Tertiary and Malm aquifers are not considered as most of the samples present typical values
433 of modern recharge from the northern Switzerland. The Keuper aquifer level mainly contain
434 young groundwaters, with detectable tritium contents, defining a relatively small range of
435 stable isotopic signatures, from -10.5 to -8.7‰ and -74 to -63‰ for $\delta^{18}\text{O}$ and $\delta^2\text{H}$
436 respectively.

437 The Muschelkalk layer first contains young waters ($^3\text{H} > 20$ TU) plotting on the meteoric
438 water line and reflecting superficial waters of the upper and middle Muschelkalk, and also
439 mixed superficial and deeper waters of the upper Muschelkalk. Samples with low tritium
440 contents ($^3\text{H} < 20$ TU) present different stable isotopes signatures, some are identical to the
441 modern samples while others are depleted in heavy isotopes or enriched in ^{18}O only. The ^{18}O
442 enriched samples correspond to hot springs, that could originate from mixing of depleted deep
443 water with enriched water in both ^2H and ^{18}O by evaporation, or by isotope exchange with the
444 rock matrix. Depleted samples in both ^2H and ^{18}O have different stories and surprisingly the
445 most depleted one, that normally must reflect an old recharge, was identified modern or
446 younger than 1 ka with dating tools. This sample, close to the Rhine River, seems to reflect a
447 recharge from the Rhine with similar signature than those of the Alpine precipitations. Some
448 other samples have signatures consistent with a recharge in cooler conditions as they were
449 estimated to older than 15-30 ka. Finally, some Muschelkalk samples probably reflect a
450 recharge in higher altitude in the adjacent Black Forest.

451 Most of the waters from the Buntsandstein, Permian and Crystalline basement are in the same
452 range for $\delta^{18}\text{O}$ and $\delta^2\text{H}$ than samples of the other upper aquifers. The 4 most depleted samples
453 from tunnels in the Alps present signatures consistent with recharge from precipitation in high
454 altitude, and thus do not reflect old waters recharged under cooler climate. Enriched waters in
455 ^2H and ^{18}O or only in ^{18}O group tritium free samples and waters with $^3\text{H} > 20$ TU as well as
456 more or less mineralized waters. They reflect a specific story, from isotope exchange due to
457 water-rock interaction to mixing of highly evaporated seawater with meteoric waters similar
458 to young waters found currently in the upper crystalline of northern Switzerland.

459 This example in Switzerland, mainly in the context of large sedimentary aquifers, illustrates
460 well that signatures of stable isotopes of the water molecule can reflect long and complex
461 stories and processes and not only climate variation through time, even when samples plot
462 along the meteoric water line. It thus evidences that isotopic data always need to be jointly
463 interpreted with chemical data in the general and local hydrogeological context.

464

465 **6 – Summary**

466 Based on the literature and recent investigations in the SW France, this study highlighted the
467 use of the isotopic methods in groundwater investigations applying stable isotopes of the
468 water molecule (hydrogen and oxygen) as tracers of water source, recharge over time and past
469 climates variations in various continental aquifers. Parameters controlling the isotopic
470 signature in rainwater (e.g. continental, altitude effects...) lead to the general relation between
471 $\delta^{18}\text{O}$ and $\delta^2\text{H}$, defined as the GMWL (Global Meteoric Water Line) and groundwater
472 generally fall along this line. If no processes affect the water molecule from surface to
473 aquifers, groundwater conditions prevailing at the moment of the recharge are preserved.
474 Thus the isotope signature may reflect recent recharge with hydrogen and oxygen isotope
475 values in the range of rainwaters or recharge under colder climate.

476 Starting from the recent study of the a multi Eocene sands layer system (five aquifers:
477 Paleocene, Eocene infra-molassic sands, early Eocene, middle Eocene, late Eocene) in the
478 Adour-Garonne district (1/5th of French territory), this study explore the recharge conditions
479 over different aquifer systems over Europe (Portugal, France, UK, Switzerland, Germany,
480 Hungary, Poland) and highlights the recharge conditions and the story of the groundwater at
481 large scale, involving recent, Holocene and Pleistocene components and eventually mixing
482 between them.

483 The Adour-Garonne district highlights the story of the recharge over different climatic
484 conditions with enriched samples in ¹⁸O and ²H that clearly correlate with the present day
485 recharge while the most depleted sample reflect an old recharge. Such processes of variable
486 recharge in aquifers over different climatic periods are also evidenced in the Aquitaine basin,
487 in the Paris Basin Chalk aquifer and in the Lorraine, Poland and Portugal Basins. Depleted
488 values in the confined part of this aquifer can be related to a lower recharge temperature at the
489 time of infiltration corresponding to Pleistocene ages.

490 In addition to this processes, the conceptual model issued from the Chalk aquifer in the
491 London Basin shows the complexity of the recharge over time and mixing processes. The
492 water evolved from connate Cretaceous marine water repeatedly mixed with fresh meteoric
493 water since the Late Tertiary, leading to the observed $\delta^{18}\text{O}$ - $\delta^2\text{H}$ variation. Such complex
494 recharge-mixing processes are also evidenced in the Germany case, in the Pannonian Basin
495 and more particularly in the example in Switzerland.

496

497 **Acknowledgements:**

498

499 This work was financially supported within the scope of the research partnership between BRGM and
500 Water Agency (Adour Garonne) through the CARISMEAU project (<http://carismeau.brgm.fr>).

501 **References**

502
503

504 [1] W.G. Darling, *Quat. Sci. Rev.* 23 (2004) 743.

505 [2] Ph. Négrel, E. Petelet-Giraud, A. Brenot, In Ph. Quevauviller, A.M. Fouillac, J. Grath &
506 R. Ward Eds., *Groundwater quality assessment and monitoring*, Wiley & Sons Ltd
507 publisher. 2009. p 331.

508 [3] P. Fritz, J.C. Fontes, *Handbook of Environmental Isotope Geochemistry*, Vol. 1 to 5.
509 1980, Elsevier Ed.

510 [4] Clark I.D. and Fritz P. 1997. *Environmental Isotopes in Hydrology*. CRC Press/Lewis
511 Publishers, 352 p.

512 [5] P.K. Aggarwal, J.R. Gat, K.F.O Froehlich, (2005). *Isotopes in the water cycle; past,*
513 *present and future of a developing science*. Springer Ed. 381pp.

514 [6] W.G. Darling, *Journal of Human Evolution*. (2011) doi:10.1016/j.jhevol.2010.05.006.

515 [7] W. Dragoni, B.S. Sukhija, in: W. Dragoni and B.S. Sukhija (eds), *Climate Change and*
516 *Groundwater*. Geological Society, London, Special Publications doi: 10.1144/SP288.1,
517 2008, 288, pp1-12.

518 [8] IPCC report, in: *IPCC Third Assessment Report - Climate Change 2001*. Accessible at
519 http://www.ipcc.ch/publications_and_data/publications_and_data_reports.shtml#1.
520 2001.

521 [9] IPCC report, in: *IPCC Fourth Assessment Report - Climate Change 2007*. Accessible at
522 http://www.ipcc.ch/publications_and_data/publications_and_data_reports.shtml#1. 2007.

523 [10] D.Z. Sun, F. Bryan, *Geophysical monograph* 189. Washington, D.C., American
524 Geophysical Union, 2010.

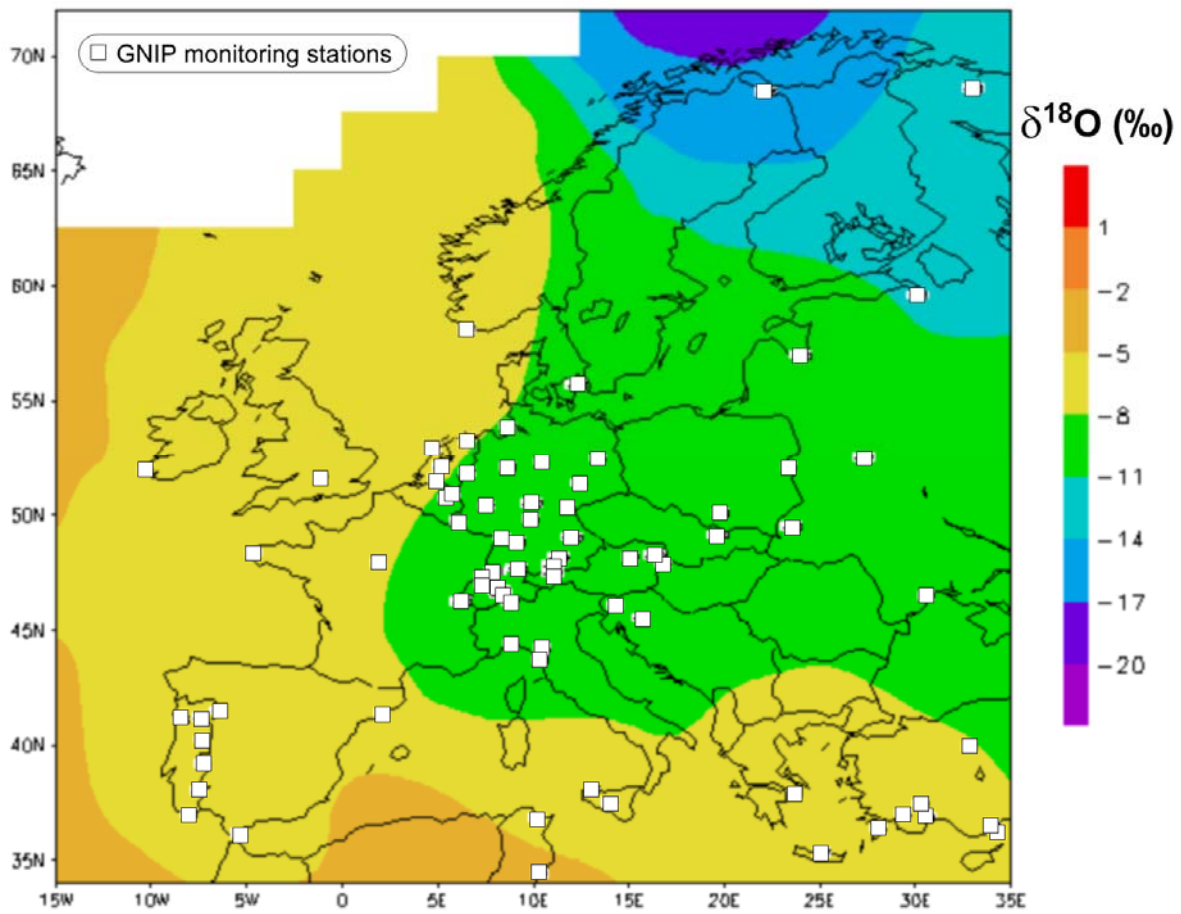
525 [11] P.A. Allen, (1997). *Earth surface processes*. Blackwell Science, 404pp.

526 [12] Hulme, M., Osborn, T.J., Johns, T.C. *Geophys. Res. Lett.* 25 (1998) 3379.

527 [13] H. Craig, *Science* 133 (1961) 1702.

- 528 [14] J.R. Gat, 1981. Groundwater. In: J.R. Gat, R. Gonfiantini (eds). Stable isotopes
529 hydrology, deuterium and oxygen 18 in the water cycle, Technical report series N°210,
530 IAEA, Vienna, 1981, 223-240.
- 531 [15] Y. Yurkstever, Worldwide survey of isotopes in precipitation. IAEA Report, Vienna.
532 1975.
- 533 [16] IAEA, GNIP Maps and Animations, International Atomic Energy Agency, Vienna. 2001.
534 Accessible at <http://isohis.iaea.org>.
- 535 [17] R. Millot, C. Guerrot, E. Petelet-Giraud, Ph. Négrel, *Appl. Geochem.* 25 (2010) 1510.
- 536 [18] W.G. Darling, J.C. Talbot, *Hydrol. Earth Syst. Sci.* 7 (2003) 163.
- 537 [19] W.G. Darling, A.H. Bath, J.C. Talbot, *Hydrol. Earth Syst. Sci.* 7 (2003) 183.
- 538 [20] A. Plata-Bedmar,. *Composicion isotopica de las precipitaciones y aguas subterraneas de*
539 *la Peninsula Iberica.* Centro des Estudios de tecnicas Aplicadas, Madrid (Spain), 1994.
540 139p.
- 541 [21] A. Longinelli, E. Selmo, *J. Hydrol.* 270 (2003) 75.
- 542 [22] A. Longinelli, E. Anglesio, O. Flora, P. Iacumin, E. Selmo, *J. Hydrol.* 329 (2006) 471.
- 543 [23] E.R.Th. Kerstel, R. van Trigt, N. Dam, J. Reuss, H.A.J. Meijer, *Anal. Chem.* 71 (1999)
544 5297.
- 545 [24] G. Lis, L.I. Wassenaar, M.J. Hendry, *Anal. Chem* 80 (2008) 287.
- 546 [25] M. Schmidt, K. Maseyk, C. Lett, P. Biron, P. Richard, T. Bariac, U. Seibt,. *Geophys.*
547 *Res. Abs.* 13 (2011) EGU2011-9375.
- 548 [26] André L. 2002. PhD Thesis, Université de Bordeaux 3. 230pp.
- 549 [27] W.M. Edmunds. In: P.K. Aggarwal, J.R. Gat, K.F.O, Froelich, (eds.), *In Isotopes and the*
550 *water cycle: past, present and future of a developing science* Springer, 2005, 341-352.
- 551 [28] C. Le Gal La Salle, C. Marlin, S. Savoye, J.C. Fontes, *Appl. Geochem.* 11 (1996) 433.

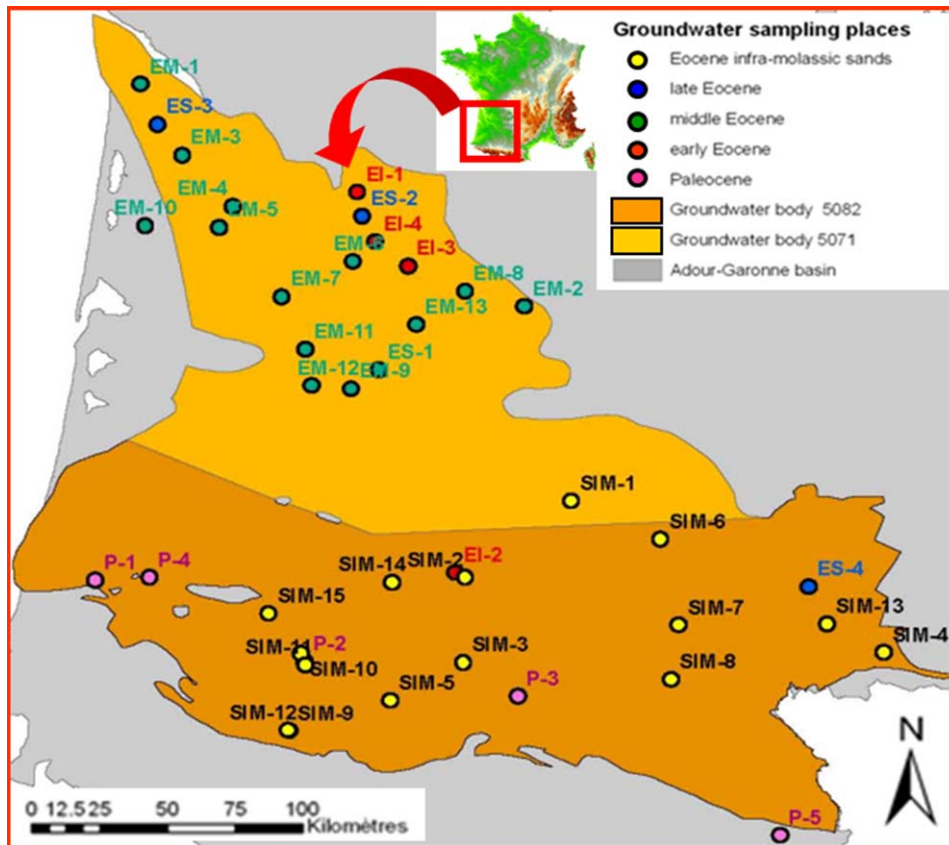
- 552 [29] H. Jirakova, F. Huneau, H. Celle-Jeanton, Z. Hrkal, P. Le Coustumer, J. Hydrol. 368
553 (2009) 1.
- 554 [30] J.M. Matray, M. Lambert, J.C. Fontes, Appl. Geochem. 9 (1994) 297.
- 555 [31] W. Kloppmann, L. Dever, W.M. Edmunds, Appl. Geochem. 13 (1998) 593.
- 556 [32] K.M. Hiscock, P.F. Dennis, P.R. Saynor, M.O. Thomas, J. Hydrol. 180 (1996) 79.
- 557 [33] F. Dennis, J.N. Andrews, A. Parker, M. Wolf, Appl. Geochem. 12 (1997) 763.
- 558 [34] T. Elliot, J.N. Andrews, W.M. Edmunds, Appl. Geochem. 14 (1999) 333.
- 559 [35] H. Celle-Jeanton, F. Huneau, Y. Travi, W.M. Edmunds, Appl. Geochem. 24 (2009)
560 1198-1213.
- 561 [36] W. Kloppmann, Ph. Négrel, J. Casanova, H. Klinge, K. Schelkes, C. Guerrot, Geochim.
562 Cosmochim. Acta 65 (2001) 4087.
- 563 [37] I. Varsanyi, J.M. Matray, L.O. Kovacs, Chem. Geol. 140 (1997) 89.
- 564 [38] A. Zuber, S.M. Weise, J. Motyka, K. Osenbruck, K. Rozanski, J. Hydrol. 286 (2004) 87.
- 565 [39] P. Galego-Fernandes, P.M. Carreira, J. Hydrol. 361 (2008) 291.
- 566 [40] F.J. Pearson, W. Balderer, H.H. Loosli, B.E. Lehmann, A. Matter, T. Peters, H.
567 Schmassmann, A. Gautschi, Studies in Environmental Science 43, Elsevier, ISBN 0-
568 444-88983-3. 1991.
- 569
570
571
572
573



574

575 **Figure 1.** Contour map of amount-weighted mean annual $\delta^{18}\text{O}$ values (‰) in precipitation
 576 derived from the GNIP database, for stations reporting as of 1997 (adapted from IAEA,
 577 [16])

578

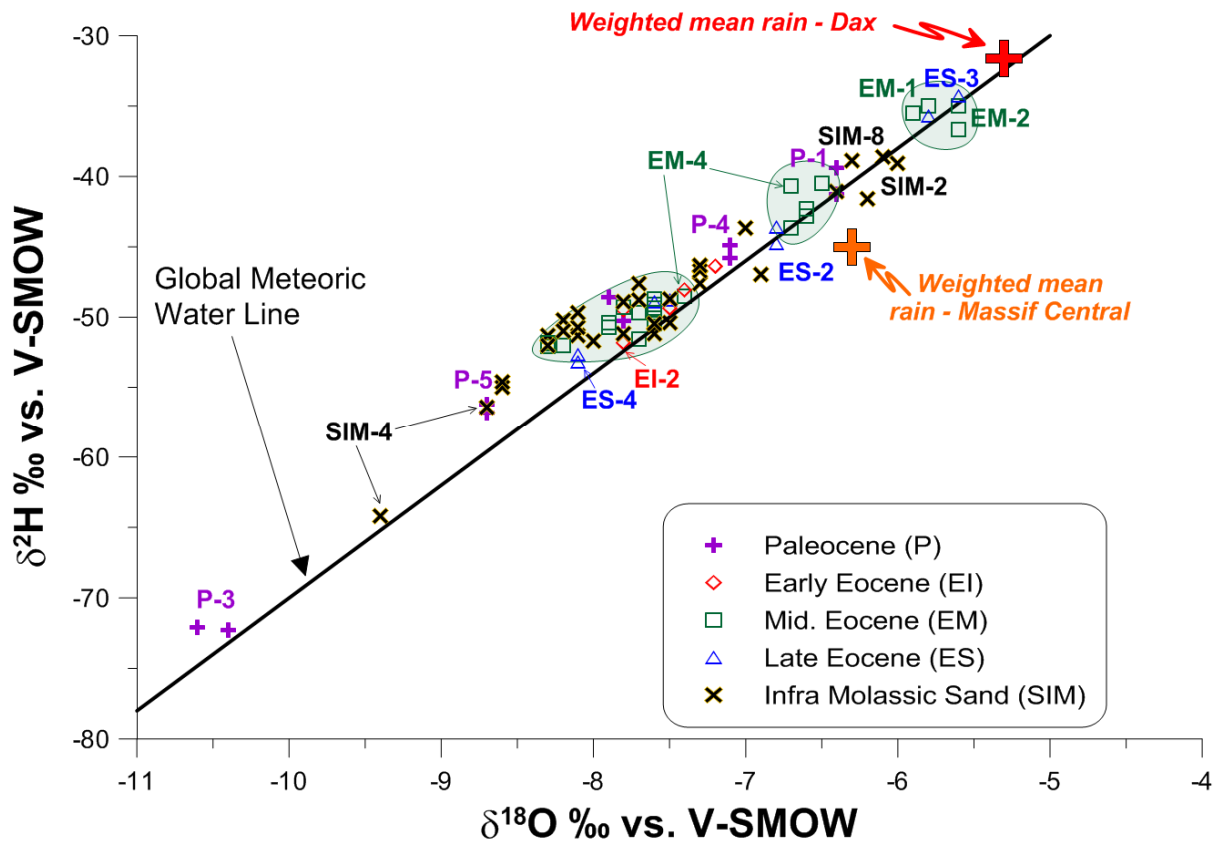


579

580 **Figure 2.** General setting of the Adour Garonne district (SW France) and schematic map of
 581 the Total Dissolved Solids (TDS, mg/l) in the IMS aquifers (adapted from [2]).

582

583



584

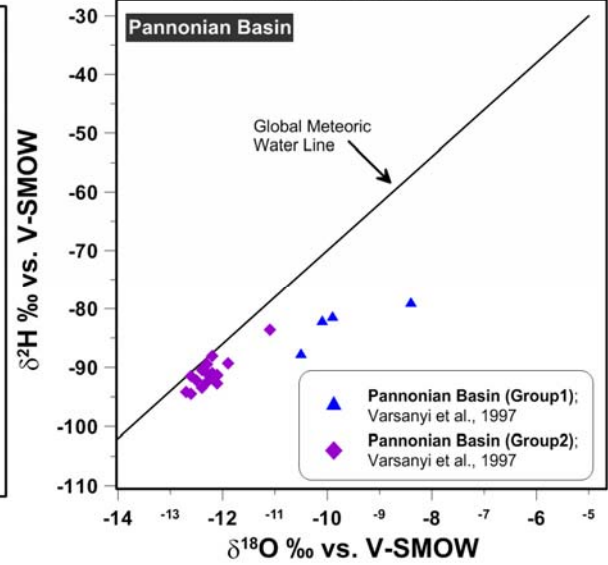
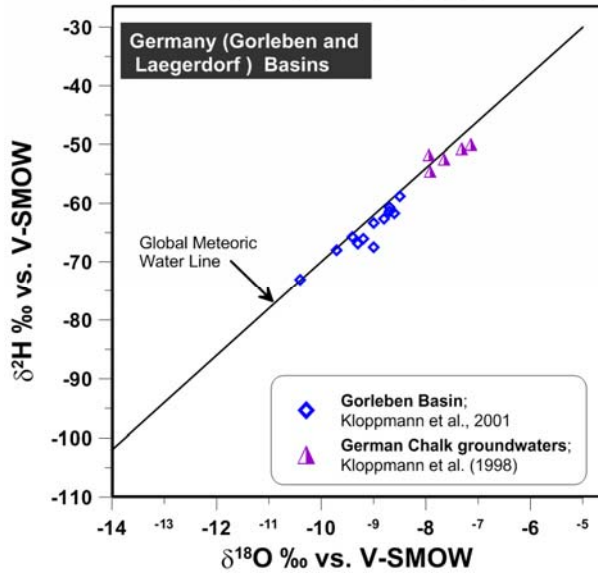
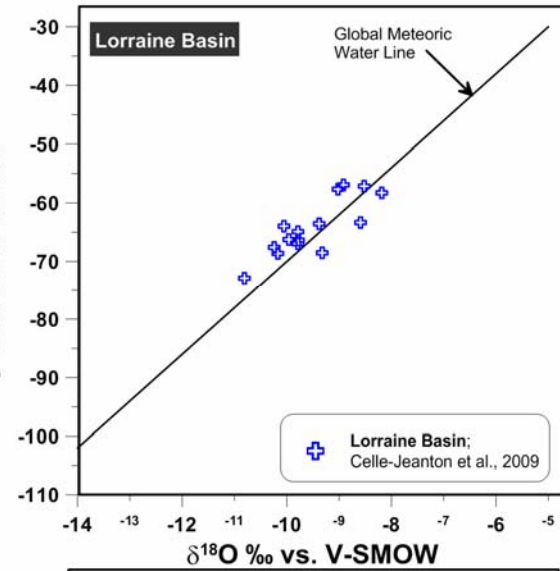
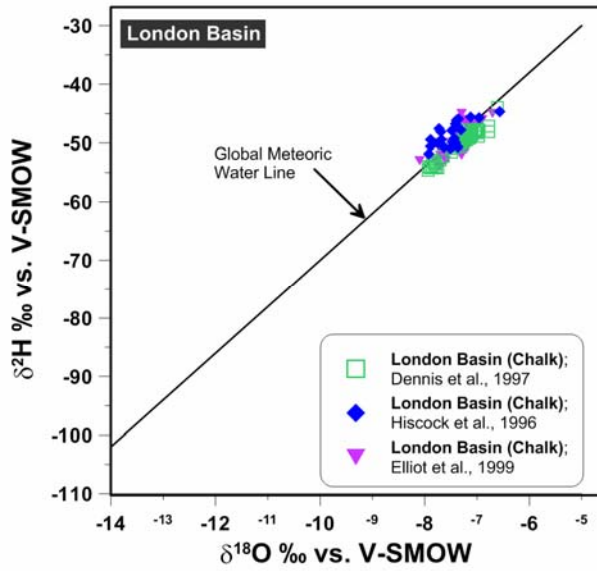
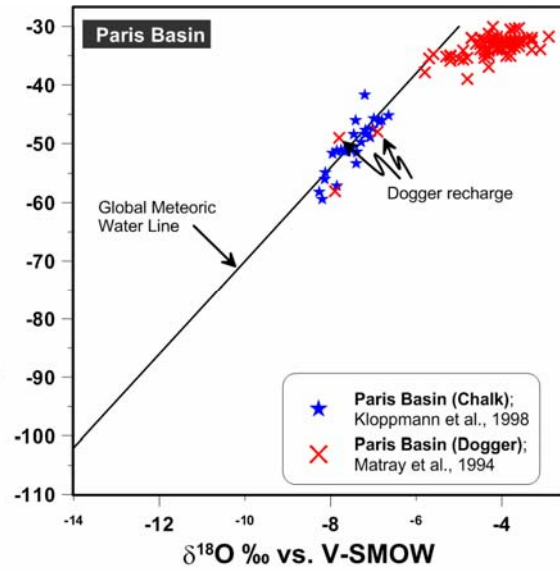
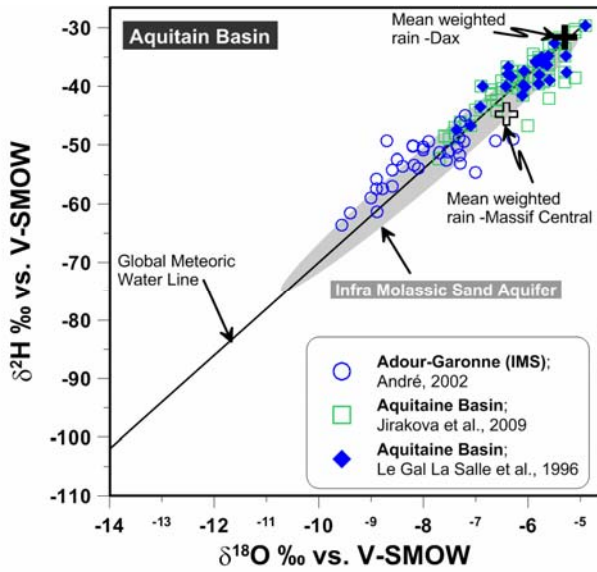
585 **Figure 3.** $\delta^{18}\text{O}$ - $\delta^2\text{H}$ plot for the ground waters collected in the Eocene sand aquifers (adapted
 586 from Négrel et al., [2]). The Global Meteoric Water Line is defined as $\delta^2\text{H} = 8 * \delta^{18}\text{O} + 10$
 587 [13].

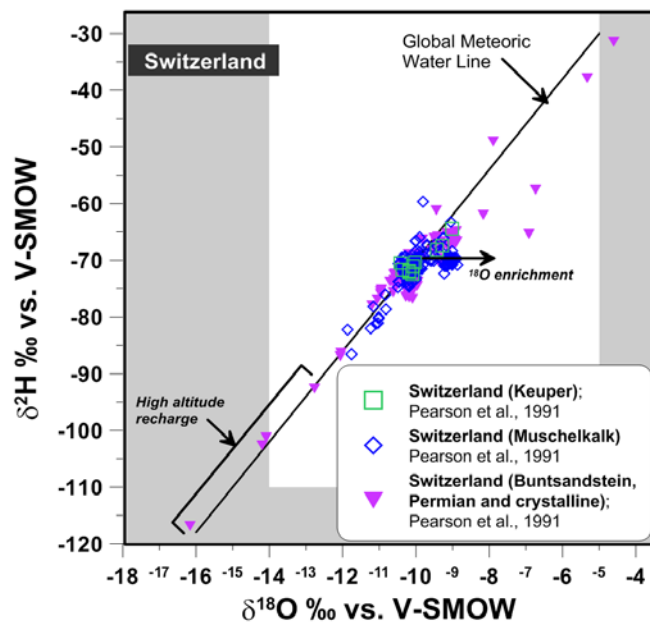
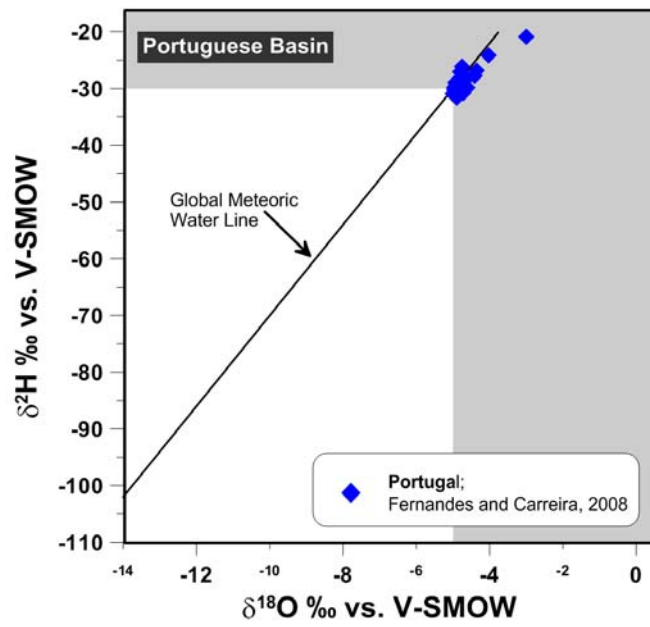
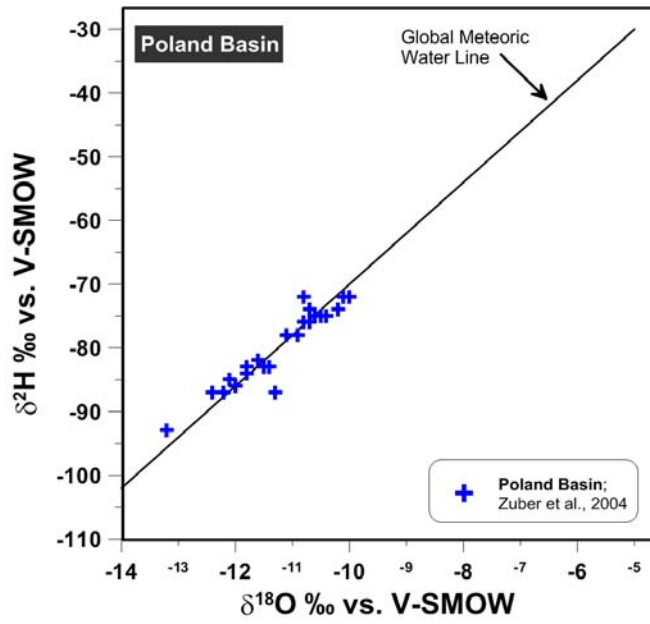
588



589
590
591

Figure 4. Location map of the main European aquifers summarized in this study.





594 **Figure 5.** $\delta^{18}\text{O}$ - $\delta^2\text{H}$ plot for the groundwaters from European aquifers; Global Meteoric
595 Water Line as in Figure 3: *Aquitaine Basin* [26, 28, 29 Data from the ground waters
596 collected in the Eocene sand aquifers are in the greyed field. Chalk aquifer from the *Paris*
597 *Basin* (data from [30, 31]. Chalk aquifer from the *London Basin* (data from [32-34).
598 *Gorleben* and Laegerdof aquifers(Germany; [31, 36). *Poland* aquifer (data from [38]).
599 *Pannonian Basin* (data from [37]). *Portugal* aquifer (data from [39]). *Switzerland* (data from
600 [40] and reference therein). *Lorraine* aquifer (Eastern France; [35]).

601

602